

# Slow surface phonon polaritons for sensing in the midinfrared spectrum

Igal Balin, Nir Dahan, Vladimir Kleiner, and Erez Hasman

Citation: *Appl. Phys. Lett.* **94**, 111112 (2009); doi: 10.1063/1.3098360

View online: <http://dx.doi.org/10.1063/1.3098360>

View Table of Contents: <http://aip.scitation.org/toc/apl/94/11>

Published by the [American Institute of Physics](#)

---

---



**Fearful for the future of science?**

Sign up for **FREE** FYI emails.

AIP | American Institute of Physics

# Slow surface phonon polaritons for sensing in the midinfrared spectrum

Igal Balin, Nir Dahan, Vladimir Kleiner, and Erez Hasman<sup>a)</sup>

Micro and Nanoptics Laboratory, Faculty of Mechanical Engineering and Russell Berrie Nanotechnology Institute, Technion–Israel Institute of Technology, Haifa 32000, Israel

(Received 8 January 2009; accepted 22 February 2009; published online 19 March 2009)

We demonstrate a reflection-type sensor in the midinfrared spectra based on resonant excitation of surface phonon polaritons (SPhPs). In this range, SPhPs are characterized by the high density of states associated with slow surface waves that lead to enhanced resonance absorption. Delocalized SPhPs were excited by irradiating TM-polarized light on a one-dimensional grating embedded in a SiC substrate. The sensor response was characterized by changing the refractive index (RI) of a lossless CO<sub>2</sub> gas. A detection limit of  $2 \times 10^{-5}$  RI units was obtained at a wavelength of 11.9  $\mu\text{m}$ . © 2009 American Institute of Physics. [DOI: 10.1063/1.3098360]

Recent technological developments have created an interest in miniature chemical and biochemical optical sensing in the midinfrared (mid-IR) (3–20  $\mu\text{m}$  wavelength) region, where most organic molecules possess vibration or rotation modes that can serve as chemical fingerprints. Indeed, a significant portion of sensing research in this spectrum relies on absorption detection methods.<sup>1,2</sup> However, another avenue that is being pursued is a refraction method, which is based on the refractive index change of the measurand, particularly in small volumes. This kind of sensing has been extensively investigated in the visible and near-IR regions and is already widespread there.<sup>3,4</sup> One of the reasons for that is the recent revival in the field of plasmonics. Sensors based on surface plasmon resonance (SPR) excitation were demonstrated by Otto<sup>5</sup> and Kretschmann<sup>6</sup> and since then there has been a considerable number of works dedicated to the development of sensing by SPR method.<sup>7</sup> Surface plasmon polaritons (SPPs) are excited by the coupling of light with collective oscillation of the conduction electrons in metals. The interaction strength corresponds to the transition probability which is known from Fermi's golden rule to be proportional to the density of states (DOS) of the surface modes ( $\text{DOS} \propto 1/v_g$ , where  $v_g = d\omega/dk$  is the group velocity of surface waves). At large wave number the frequency of the surface waves approaches a characteristic SPP frequency  $\omega_{\text{SPP}}$  ( $\omega_{\text{SPP}} = \omega_p / \sqrt{2}$  at metal-vacuum interface, where  $\omega_p$  is the plasma frequency), as shown in Fig. 1(a). Near the SPP frequency (in the visible or near-IR regions), the delocalized SPPs are characterized by a high DOS, thus significant absorption is obtained. On the other hand, far from the SPP frequency (in the mid-IR region), delocalized SPPs are characterized by a low DOS resulting in weak absorption. Several mechanisms were proposed to increase the DOS by changing the dynamics of the delocalized surface waves. These changes can be due to tailoring the plasma frequency within a metamaterial,<sup>8</sup> localization of SPPs in microcavities,<sup>9</sup> surface enhanced infrared absorption,<sup>10</sup> confined waveguiding plasmonic modes in ultrathin film,<sup>11</sup> plasmonic bandgap structure,<sup>12</sup> and standing waves coupled SPPs.<sup>13</sup>

In this letter, we propose utilizing a different type of surface waves known as surface phonon polaritons (SPhPs) for refractive index sensing in the mid-IR region. SPhPs

arise from the interaction of an electromagnetic field with the optical phonons in polar dielectrics. Typically, the SPhP frequency (the asymptotic frequency at large wave number) is in the IR region [see Fig. 1(a)], hence in this spectral range *delocalized* SPhPs are characterized by a high DOS corresponding to slow waves. The high DOS of surface waves in the mid-IR was recently investigated to obtain a resonant

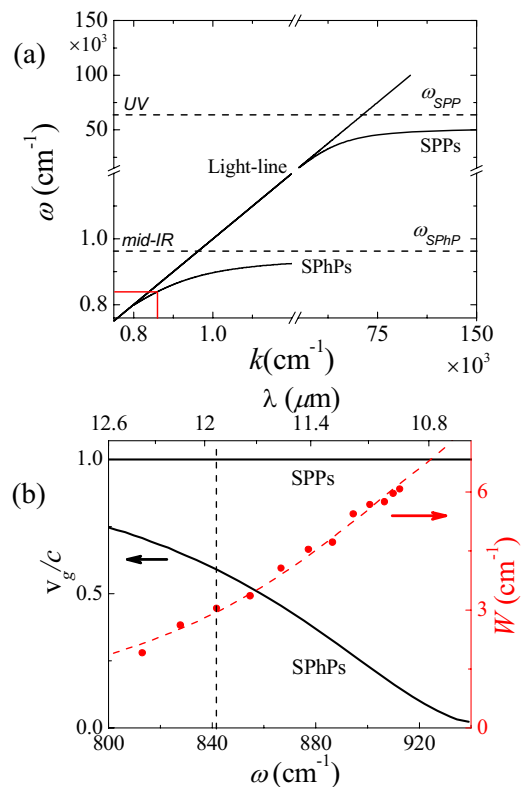


FIG. 1. (Color online) (a) Dispersion relation of SPPs in metal (Au) and SPhPs in polar material (SiC), dielectric constants taken from Ref. 19 for Au and Ref. 16 for SiC. Dashed lines represent the SPP frequency ( $\omega_{\text{SPP}}$ ) and the SPhP frequency ( $\omega_{\text{SPhP}}$ ) which are in the ultraviolet and in the mid-IR spectrum, respectively. Red solid line represents the resonance frequency for which our element was designed. (b) Group velocity of delocalized SPPs and SPhPs normalized by the speed of light in vacuum, along with calculated dip width: red dash line—derived from the imaginary part of the frequency; circles—calculated by RCWA (each resonance frequency was matched with an appropriate grating according to the momentum matching condition). The dashed line represents the resonance frequency (wavelength) for which our element was designed.

<sup>a)</sup>Electronic mail: mehasman@tx.technion.ac.il.

thermal emission.<sup>14,15</sup> Herein, we exploit this mechanism for absorption, which turns out to be a promising candidate for sensing in the IR region. We investigate theoretically and experimentally a reflection-type sensor based on a wavelength scanning method. Our sensing element consists of a grating embedded in a SiC substrate in which excitation of delocalized SPhPs was achieved by illumination with TM-polarized light. We characterized the sensor response by the refractive index changes in the environment near 11.9  $\mu\text{m}$  wavelength (corresponding to  $\omega_0 \approx 840 \text{ cm}^{-1}$ ) by varying the pressure of a lossless  $\text{CO}_2$  gas. A detection limit of  $2 \times 10^{-5}$  refraction index unit (RIU) was achieved.

SPhPs are excited in SiC in a spectral range for which the real part of its dielectric constant is smaller than  $-1$  (10.6–12.5  $\mu\text{m}$  wavelength).<sup>16</sup> Their dispersion relation on a smooth surface is given by  $k_{\parallel} = k_0 \sqrt{\varepsilon_s \varepsilon_a / (\varepsilon_s + \varepsilon_a)}$ ,<sup>17</sup> where  $k_0$  is the wave number of the incident wave in a vacuum, and  $\varepsilon_s$  and  $\varepsilon_a$  are the substrate and the ambient dielectric constants, respectively. Figure 1(a) shows the dispersion relation of SPhPs on a SiC/vacuum interface along with SPPs on a metal/vacuum interface, such as with gold. As can be seen, the SPP and SPhP frequencies ( $\omega_{\text{SPP}}$  and  $\omega_{\text{SPhP}}$ ) are obtained from the resonant excitation condition  $\varepsilon_s = -\varepsilon_a$  are in the ultraviolet/visible and mid-IR regions, respectively. From this relation one can find the group velocity of surface waves on SiC and gold versus frequency, as shown in Fig. 1(b). In the vicinity of 11.9  $\mu\text{m}$  wavelength, slow waves of SPhPs ( $v_g = 0.6c$ ) are observed compared with the group velocity of the SPPs ( $v_g \approx c$ ). Thus, the small group velocity of the surface waves which is inversely proportional to the high DOS ensures high coupling efficiency. Furthermore, the interaction length of SPhPs within the ambience is estimated according to their penetration depth  $L_a \approx 1/\text{Im}(\sqrt{\varepsilon_a k_0^2 - k_{\parallel}^2})$ ,<sup>17</sup> which is of the order of the incident wavelength,  $L_a = 8.32 \mu\text{m}$  at 11.9  $\mu\text{m}$  wavelength. These allow us to measure the refractive index changes in the measurand in a small volume, which has a potential to implement this technique in integrated sensor devices. This interaction length is much smaller than the desired sample cell length required for conventional refractive index sensing methods in the mid-IR, for example, interferometer technique.<sup>18</sup> In this technique, the sample cell is of the order of 0.5 m for measuring a change of  $10^{-5}$  RIU at 10  $\mu\text{m}$  wavelength.

We performed experiments on a 10 mm square grating fabricated by a standard photolithographic technique using reactive ion etching.<sup>15</sup> A setup illustration of the reflection measurement is shown in Fig. 2(a), and a scanning electron microscope image of the realized structure is given in Fig. 2(b) having the following profile parameters: periodicity  $\Lambda = 11.6 \mu\text{m}$ , fill factor  $q = 0.6$ , and depth  $h = 0.3 \mu\text{m}$ . The periodicity of the grating was chosen so that the resonance frequency  $\omega_0$  would be absorbed at a normal incident angle, following the momentum matching condition  $k_0 \sqrt{\varepsilon_a} \sin \theta + mK_g = k_{\parallel}$ .<sup>17</sup>  $\theta$  denotes the incident angle  $m$  is the diffraction order and  $K_g = 2\pi/\Lambda$  is the grating wave number.

First, we characterized the sensor by calculating the spectral reflectivity of the structure using a rigorous coupled wave analysis (RCWA) method for an ambient refractive index change of  $\Delta n = 4.3 \times 10^{-4}$  RIU. Figure 3(a) summarizes the resonance spectral shift normalized by the resonance frequency in a vacuum  $(\omega - \omega_0)/\omega_0$ , as a function of the refractive index change  $\Delta n$ . A typical resonant dip is shown in the

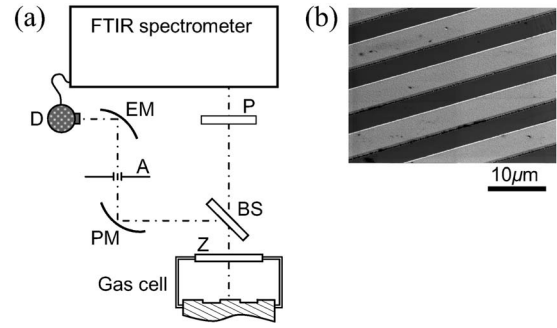


FIG. 2. (a) Experimental setup used for measurement of the spectral reflectivity. P denotes polarizer, BS denotes beam-splitter, Z denotes ZnSe window with an antireflection coating, PM denotes parabolic mirror, focal length 180 mm, EM denotes elliptic mirror, focal lengths 42 /280 mm, A denotes angular resolution aperture, diameter 0.8 mm, and D denotes HgCdTe detector. (b) Scanning electron microscope image of the realized structure.

inset at  $\Delta n = 3 \times 10^{-4}$  RIU with a dip width at half maximum  $3.15 \text{ cm}^{-1}$ . The spectral sensitivity  $S_\omega = (\omega - \omega_0)/\Delta n$  can be derived from the slope of the curve to be  $S_\omega = 625 \text{ cm}^{-1}/\text{RIU}$ . Our sensing element was inserted into a gas chamber to determine the variation of the  $\text{CO}_2$  refractive index that results from variations in the gas pressure (from 0.97 to 0.02 atm in steps of  $0.16 \pm 0.013 \text{ atm}$ ). Measurement of the reflection spectra was performed using a Fourier transform infrared spectrometer (Bruker Vertex 70) equipped with an HgCdTe detector. Each measurement was obtained by averaging 128 scans with a spectral resolution of  $0.5 \text{ cm}^{-1}$ , and an angular resolution of  $0.1^\circ$ , which is much smaller than the angular lobe at the resonance frequency ( $\sim 1^\circ$ ). A typical experimental result at  $p = 0.33 \text{ atm}$  is shown in the inset of Fig. 3(b) with a dip width at half maximum  $8.49 \text{ cm}^{-1}$ . As can be seen from our results, the measured dip width is wider than the calculated one. We attribute this broadening to carbon impurities in our SiC sample. The dip shape is well fitted to a truncated Lorentzian-shape in which its resonance frequency overlaps with its geometric center of mass position. This property was utilized to find the measured dip position using the centroid method. Figure 3(b) shows the experimental results of the resonant spectral shift normalized by the resonance frequency in a vacuum as a function of the  $\text{CO}_2$  gas pressure. In order to estimate the uncertainty of the dip position, we calculated the minimum spectral change that can be detected by the centroid method,  $\delta\omega = K(W/d) \times (\sigma_{\text{th}}/\sqrt{N})$ .<sup>7</sup> Our experimental results yielded  $\delta\omega = 0.0105 \text{ cm}^{-1}$ , where  $\sigma_{\text{th}} = 0.0058$  is the measured noise at a threshold level which was set at half of the dip height,  $d = 0.37$  is the depth of the dip with respect to the threshold,  $W = 8.49 \text{ cm}^{-1}$  is the width of the dip at the threshold [see inset in Fig. 3(b) for details],  $N = 40$  is the number of measured points beneath the threshold, and  $K \approx 0.5$  stands for the noise involved in the detection system.

Using the calculated curve in Fig. 3(a) with the experimental data in Fig. 3(b), we can deduce a relation between the refractive index of  $\text{CO}_2$  gas and its pressure  $\Delta n \approx \alpha p$ , where  $\alpha = 4.034 \times 10^{-4} \text{ atm}^{-1}$  [see Fig. 3(c)]. This value is in a good agreement with other experimental results on  $\text{CO}_2$  gas  $\alpha = 4.087 \text{ atm}^{-1}$  obtained by a differential interferometer technique as well as with theoretical calculation  $\alpha = 4.065 \times 10^{-4} \text{ atm}^{-1}$  at 10.6  $\mu\text{m}$  wavelength. The theoretical value was obtained using a Lorentz–Lorenz relation under the as-

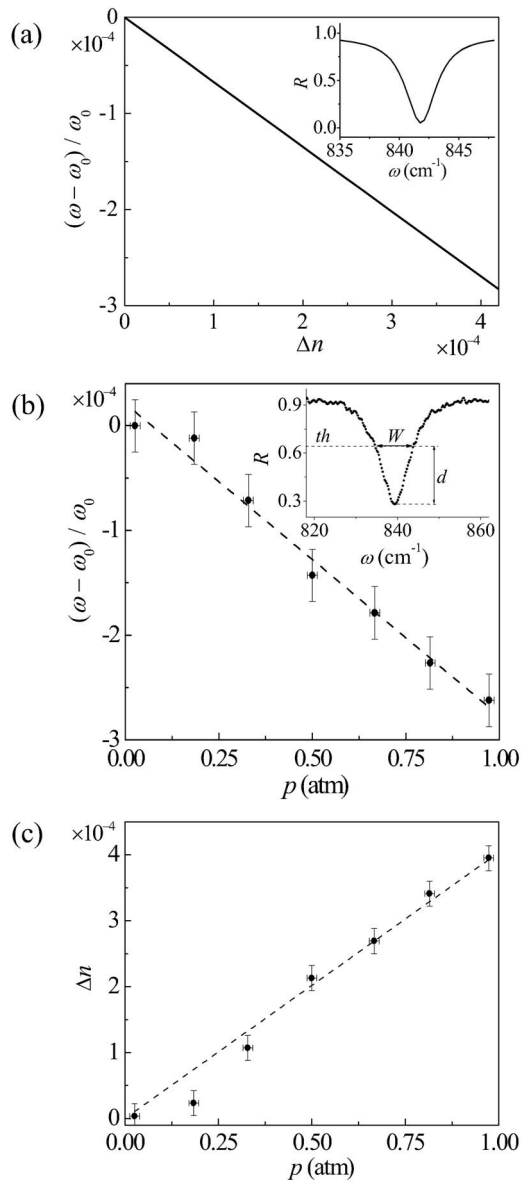


FIG. 3. (a) Normalized resonance frequency shift as a function of RI difference of the ambient calculated by RCWA. A typical spectral reflectivity for  $\Delta n = 3 \times 10^{-4}$  is shown in the inset. (b) Normalized resonance frequency shift vs pressure of  $\text{CO}_2$  gas, measurements (circles) and linear fit (dashes). The inset depicts typical reflectivity measurements at  $p = 0.33$  atm. (c) Calibration of  $\text{CO}_2$  refractive index changes vs pressure obtained from the calculation in Fig. 3(a) and the experimental data in Fig. 3(b).

sumption that  $\text{CO}_2$  behaves as an ideal gas at low pressures and Drude–Lorentz equation extended to several oscillators at atmospheric pressure (see Ref. 18 and the references therein). The foregoing calibration enables us to calculate the refractive index resolution by  $\delta n = \delta\omega / S_\omega = 2 \times 10^{-5}$  RIU. Note that  $\delta n \propto W/d$ , therefore reducing the experimental width  $W$  or deepening the dip  $d$  will increase the sensor's resolution. The dip depth is associated with the strength of interaction corresponding to slow SPhPs. For this reason, we felt directed to sense at frequencies near the SPhP frequency.

However, in this range the short decay time of the surface modes broadens the spectral dip where the dip width can be estimated via the imaginary part of the frequency  $\omega'' \propto 1/\tau \propto W$ .<sup>17</sup> The decay time and the propagation length along the surface are correlated by  $L_{\parallel} = \tau v_g$ , whereas  $L_{\parallel} \approx 1/k_{\parallel}''$  ( $k_{\parallel}''$  is the imaginary part of  $k_{\parallel}$ ). The trade-off between the group velocity of the slow SPhPs and the dip width is shown in Fig. 1(b) where  $W \approx \omega'' \approx \pi v_g k_{\parallel}''$ . An excellent agreement is obtained comparing this value with the dip width calculated by RCWA. Thus, in order to achieve a high resolution, the slow SPhPs should be used for enhanced absorption but not at frequencies too close to the SPhP frequency, such that losses in the substrate are dominant. In our SiC sample, the sensing dynamic range with high resolution is at frequencies with  $v_g > 0.2c$ .

In conclusion, we have demonstrated a sensor for a refractive index measurement in the mid-IR spectra based on slow SPhPs. The sensitivity was verified using  $\text{CO}_2$  gas at different pressures which simulated tiny changes in the environment refractive index. Sensing by SPhPs is not exclusive to gaseous environments; it may be successfully employed in liquids, soft matter, and biomolecules. The proposed concept can be extended to the far-IR region by using other polar materials that support SPhPs, e.g., GaAs (34.2–37.2  $\mu\text{m}$ ), CdTe (59.1–70.9  $\mu\text{m}$ ), or PbSe (49.2–256.5  $\mu\text{m}$ ).

This research was supported by the Israel Science Foundation.

- <sup>1</sup>Y. Raichlin, L. Fel, and A. Katzir, *Opt. Lett.* **28**, 2297 (2003).
- <sup>2</sup>S. E. Plunkett, S. Propst, and M. S. Braiman, *Appl. Opt.* **36**, 4055 (1997).
- <sup>3</sup>N. Skivesen, R. Horvath, and H. C. Pedersen, *Opt. Lett.* **30**, 1659 (2005).
- <sup>4</sup>D. F. Dorfner, T. Hürlimann, T. Zabel, L. H. Frandsen, G. Abstreiter, and J. J. Finley, *Appl. Phys. Lett.* **93**, 181103 (2008).
- <sup>5</sup>A. Otto, *Z. Phys.* **216**, 398 (1968).
- <sup>6</sup>E. Kretschmann, *Z. Phys.* **241**, 313 (1971).
- <sup>7</sup>J. Homola, *Chem. Rev. (Washington, D.C.)* **108**, 462 (2008).
- <sup>8</sup>J. B. Pendry, L. Martin-Moreno, and F. J. Garcia-Vidal, *Science* **305**, 847 (2004).
- <sup>9</sup>H. T. Miyazaki and Y. Kurokawa, *Phys. Rev. Lett.* **96**, 097401 (2006).
- <sup>10</sup>A. Hartstein, J. R. Kirtley, and J. C. Tsang, *Phys. Rev. Lett.* **45**, 201 (1980).
- <sup>11</sup>V. Lirtsman, R. Ziblat, M. Golosovsky, D. Davidov, R. Pogreb, V. Sacks-Graneck, and J. Rishpon, *J. Appl. Phys.* **98**, 093506 (2005).
- <sup>12</sup>G. Biener, N. Dahan, A. Niv, V. Kleiner, and E. Hasman, *Appl. Phys. Lett.* **92**, 081913 (2008).
- <sup>13</sup>M. B. Sobnack, W. C. Tan, N. P. Wanstall, T. W. Preist, and J. R. Sambles, *Phys. Rev. Lett.* **80**, 5667 (1998).
- <sup>14</sup>J.-J. Greffet, R. Carminati, K. Joulain, J.-P. Mulet, S. Mainguy, and Y. Chen, *Nature (London)* **416**, 61 (2002).
- <sup>15</sup>N. Dahan, A. Niv, G. Biener, Y. Gorodetski, V. Kleiner, and E. Hasman, *Phys. Rev. B* **76**, 045427 (2007); N. Dahan, A. Niv, G. Biener, Y. Gorodetski, V. Kleiner, and E. Hasman, *ASME J. Heat Transfer* **130**, 112401 (2008).
- <sup>16</sup>E. D. Palik, *Handbook of Optical Constants of Solids* (Academic, Orlando, 1985).
- <sup>17</sup>H. Raether, *Surface Plasmons on Smooth and Rough Surfaces and on Gratings* (Springer, Berlin, 1988).
- <sup>18</sup>S. Marchetti and R. Simili, *Infrared Phys. Technol.* **47**, 263 (2006).
- <sup>19</sup>M. A. Ordal, L. L. Long, R. J. Bell, S. E. Bell, R. R. Bell, R. W. Alexander, Jr., and C. A. Ward, *Appl. Opt.* **22**, 1099 (1983).